Electronic Supplementary information

Conversion of *n*-butane and product selectivity was calculated from mole fraction of products in outflow as below :

$$Conversion\ of\ n-butane\ (\%) = \frac{([C_4H_{10}]_{in} - [C_4H_{10}]_{out})}{[C_4H_{10}]_{in}} \times 100 \quad \ldots\ldots\ldots\ldots\ldots\ldots\ldots\ldots \quad (1)$$

$$Conversion\ of\ oxidant\ (\%) = \frac{([oxidant]_{in} - [oxidant\ ]_{out})}{[oxidant]_{in}} \times 100 \quad \ldots\ldots\ldots\ldots\ldots\ldots\ldots\ldots \quad (2)$$

$$Selectivity\ (\%) = \frac{moles\ of\ the\ product}{total\ moles\ of\ the\ product} \times 100 \quad \ldots\ldots\ldots\ldots\ldots\ldots\ldots\ldots\ldots\ldots\ldots\ldots \quad (3)$$

1. Mass and Heat Transfer Calculations for n-butane oxidation over Ni-Mo/Al_2O_3 catalyst

Mears Criterion for External Diffusion (Fogler, p841; Mears, 1971)

n-butane activation over oxygen:

If $\frac{-r_A'\rho_b Rn}{k_c C_{Ab}} < 0.15$, then external mass transfer effects can be neglected.

$-r_A'$ = reaction rate, kmol/kg-cat · s = 4.98 x 10^{-5} kmol-C_3/kg-cat . s

n = reaction order = 2

R = catalyst particle radius, m=3 x 10^{-5} m

ρ_b = bulk density of catalyst bed, kg/m^3

=(1-ϕ) (ϕ= porosity or void fraction of packed bed)= 1024 kg/m^3

ρ_c = solid catalyst density, kg/m^3= 1.28 m/s

C_{Ab} = bulk gas concentration of A, kmol/m^3 = 0.0075 kmol/m^3

k_c = mass transfer coefficient, m/s = 1.28 m/s

$$\frac{-r_A'\rho_b Rn}{k_c C_{Ab}} = \mathbf{3.12 \times 10^{-4} < 0.15}$$ **{Mears for External Diffusion}**

Similarly, for CO_2 = 2.85 x 10^{-4} and for N_2O = 1.72 x 10^{-4}

2. Weisz-Prater Criterion for Internal Diffusion (Fogler, p839)

If $C_{WP} = \dfrac{-r'_{A(obs)}\rho_c R^2}{D_e C_{As}} < 1$, then internal mass transfer effects can be neglected.

$-r'_{A(obs)}$ = observed reaction rate, kmol/kg-cat · s = 5.05 x 10^{-5} kmol-C_3/kg-cat . s

R = catalyst particle radius, m =3 x 10^{-5} m

ρ_c = solid catalyst density, kg/m^3 = 3600 kg/m^3

D_e = effective gas-phase diffusivity, m^2/s **[Fogler, p815]**

$$= \frac{D_{AB}\phi_p\sigma_c}{\tau}$$ where

D_{AB} = gas-phase diffusivity m^2/s; ϕ_p = pellet porosity; σ_c =constriction factor; τ =tortuosity.

C_{As} = gas concentration of A at the catalyst surface, kmol-A/m^3 = 0.0041 kmol-C3/m^3

$$C_{WP} = \frac{-r'_{A(obs)}\rho_c R^2}{D_e C_{As}} = \mathbf{4.9 \times 10^{-4} < 1}$$ **{Weisz-Prater Criterion for Internal Diffusion}**

Similarly, for CO_2 = 4.07 x 10^{-4} and for N_2O = 2.28 x 10^{-4}

3. Mears Criterion for Combined Interphase and Intraparticle Heat and Mass Transport (Mears, 1971)

$$\frac{-r'_A R^2}{C_{Ab}D_e} < \frac{1+0.33\gamma\chi}{|n-\gamma_b\beta_b|(1+0.33n\omega)}$$

$$\gamma = \frac{E}{R_g T_s};\ \gamma_b = \frac{E}{R_g T_b};\ \beta_b = \frac{(-\Delta H_r)D_e C_{Ab}}{\lambda T_b};\ \chi = \frac{(-\Delta H_r)-r'_A R}{h_t T_b};\ \omega = \frac{-r'_A R}{k_c C_{Ab}}$$

γ = Arrhenius number; β_b = heat generation function;

λ = catalyst thermal conductivity, W/m.K;

χ = Damköhler number for interphase heat transport

ω = Damköhler number for interphase mass transport

$\frac{-r'_A R^2}{C_{Ab} D_e}$ **= 3.11 x10^{-5} < 3{Mears Criterion for Interphase and Intraparticle Heat and Mass Transport }**

Similarly, for CO_2 = 2.15 x 10^{-5} and for N_2O = 1.72 x 10^{-5}

Table S1: The effect of metal oxide, support and promoter on the *n*-butane oxidative activation

Catalyst	***n*-butane conversion (mol %)**	**Oxidant**	**Temperature**	**TOF (s^{-1})**	**Reference**
7 % V_2O_5/SiO_2	1.2	Air	230	0.4 x 10^{-5}	[1, 2]
17.5 % V_2O_5/Al_2O_3	7.2	Air	230	0.9 x 10^{-5}	[1, 2]
6 % V_2O_5/Nb_2O_5	17.3	Air	230	3.6 x 10^{-5}	[1, 2]
4 % V_2O_5/ZrO_2	16.0	Air	230	4.5 x 10^{-5}	[1]
3 % V_2O_5/CeO_2	10.6	Air	230	6.3 x 10^{-5}	[1]
5 % V_2O_5/TiO_2	27.8	Air	230	19.6 x 10^{-5}	[1]
1 % V_2O_5/ 5 % P_2O_5/TiO_2	12.1	Air	230	27.0 x 10^{-5}	[1]
6 % WO_3/ 1 % V_2O_5/TiO_2	23.6	Air	230	34.1 x 10^{-5}	[1]
γ-Bi_2MoO_6	30.2	Air+steam	420	43.6 x 10^{-4}	[3]
β-$Bi_2Mo_2O_9$	39.8	Air+steam	320	57.8 x 10^{-4}	[3]
$BiMoZr_x$ oxide	42.3	Air	440	6.11 x 10^{-4}	[4]
$BiMoFe_x$ oxide	68.6	Air	420	9.23 x 10^{-4}	[5]
$ZrFe_{2-x}Al_xO_4$	55.1	Air	420	7.96 x 10^{-4}	[6]
$ZnFe_2O_4$	41.3	Air	420	5.97 x 10^{-4}	[3, 7]
TiP_2O_7-M1	24.0	CO_2	530	3.47 x 10^{-4}	[8]
TiP_2O_7-M2	22.3	CO_2	530	3.22 x 10^{-4}	[8]
1.2 % Cr 2.8 %	10.2	CO_2	550	1.47 x 10^{-4}	[9]

V/MCM-41					
1.2 % Cr 2.8 % V/ZSM-5	8.3	CO_2	550	1.20×10^{-4}	[9]
1.2 % Cr 2.8 % V/ MCM-22	7.2	CO_2	550	1.04×10^{-4}	[9]
1.2 % Cr 2.8 % V/ZSM-5(Mesoporus)	6.1	CO_2	550	8.81×10^{-5}	[9]

XPS analysis of fresh reduced and reoxidised catalyst:

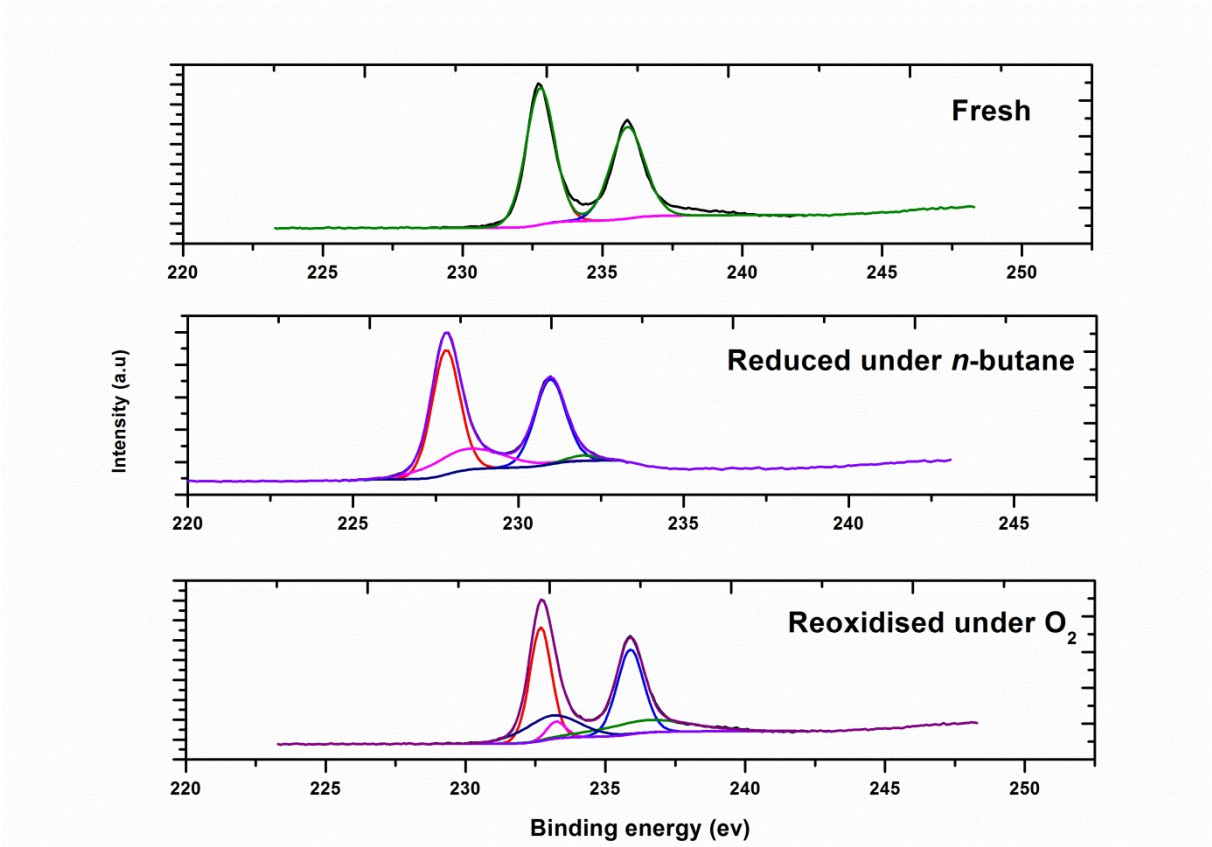

Figure S1: X-ray photoelectron spectra (Mo 3d - S 2s region) of $NiMo/Al_2O_3$ catalysts Reduced and and reoxidised samples are included for comparison

4. Kinetics of reduction and oxidation:

The kinetics of reduction and oxidation was calculated using Autochem 2920 Chemisorption analyser. A series of reduction (TPR) and oxidation (TPO) experiments (as explained in Experimental section) were done at different heating rates namely 2 °C/min, 5 °C/min, 7 °C/min, 10 °C/min, 14 °C/min and 20 °C/min. The data are plotted and the slope determined to calculate the rate, activation energy for reduction and oxidation [10].

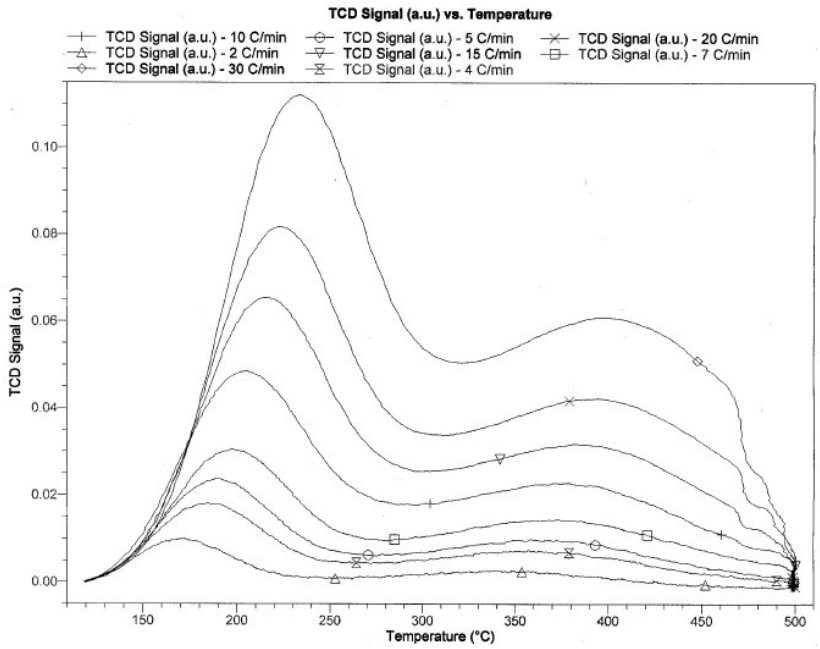

Figure S2: First order kinetics of reduction experiments of Ni-Mo/Al_2O_3 catalyst

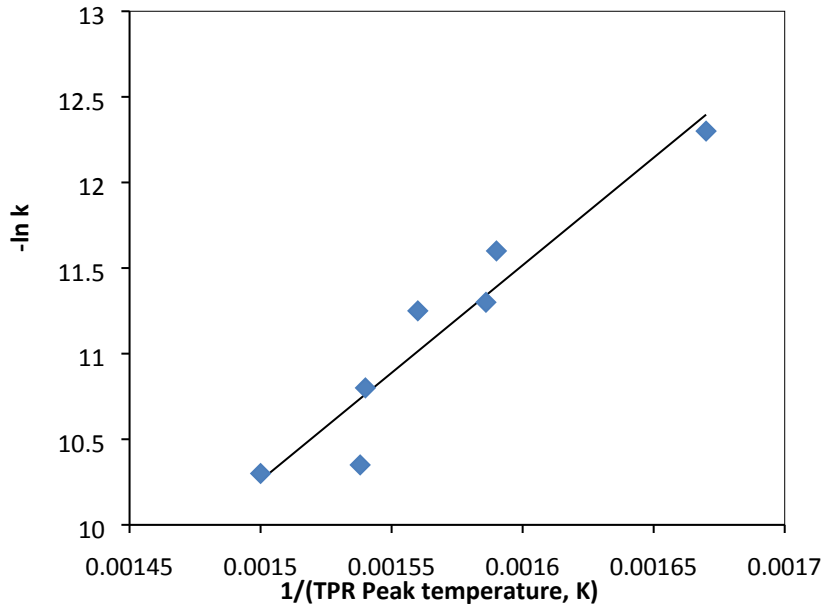

Figure S3: Arrhenius relationship profile of reduction (with H_2) of Ni-Mo/Al_2O_3 catalyst

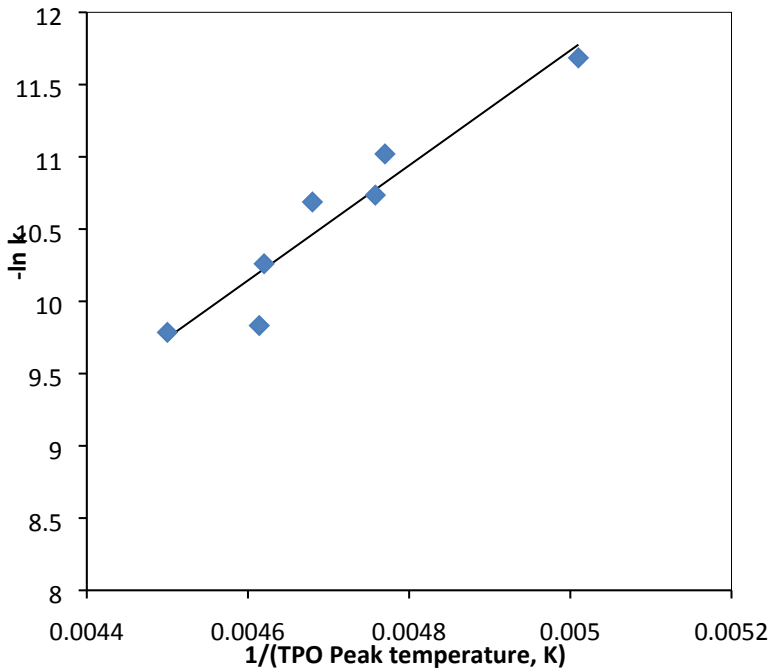

Figure S4: Arrhenius relationship profile of oxidation (with O_2) of Ni-Mo/Al_2O_3 catalyst

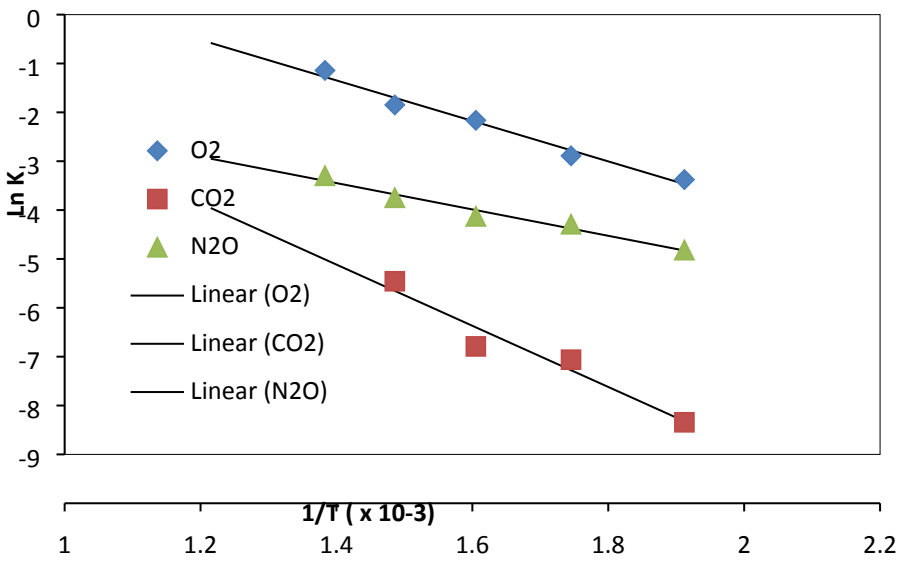

Figure S5: Arrhenius relationship profile of *n*-butane activation over different oxidants

References

[1] I.E. Wachs, J.-M. Jehng, G. Deo, B.M. Weckhuysen, V.V. Guliants, J.B. Benziger, S. Sundaresan, Fundamental Studies of Butane Oxidation over Model-Supported Vanadium Oxide Catalysts: Molecular Structure-Reactivity Relationships, J. Catal., 170 (1997) 75-88.

[2] I.E. Wachs, J.-M. Jehng, G. Deo, B.M. Weckhuysen, V.V. Guliants, J.B. Benziger, In situ Raman spectroscopy studies of bulk and surface metal oxide phases during oxidation reactions, Catal. Today, 32 (1996) 47-55.

[3] J.C. Jung, H. Kim, A.S. Choi, Y.-M. Chung, T.J. Kim, S.J. Lee, S.-H. Oh, I.K. Song, Effect of pH in the preparation of γ-Bi2MoO6 for oxidative dehydrogenation of n-butene to 1,3-butadiene: Correlation between catalytic performance and oxygen mobility of γ-Bi2MoO6, Catal. Commun., 8 (2007) 625-628.

[4] R. Grasselli, Fundamental Principles of Selective Heterogeneous Oxidation Catalysis, Top. Catal., 21 (2002) 79-88.

[5] J.-H. Park, C.-H. Shin, Oxidative dehydrogenation of butenes to butadiene over Bi–Fe–Me(Me = Ni, Co, Zn, Mn and Cu)–Mo oxide catalysts, J Ind. Eng. Chem., 21 (2015) 683-688.

[6] J.A. Toledo, P. Bosch, M.A. Valenzuela, A. Montoya, N. Nava, Oxidative dehydrogenation of 1-butene over Zn□Al ferrites, J. Mol. Catal. A: Chem., 125 (1997) 53-62.

[7] Y.-M. Chung, Y.-T. Kwon, T.J. Kim, S.J. Lee, S.-H. Oh, Prevention of Catalyst Deactivation in the Oxidative Dehydrogenation of n-Butene to 1,3-Butadiene over Zn-Ferrite Catalysts, Catal. Lett., 131 (2009) 579-586.

[8] I.-C. Marcu, I. Sandulescu, J.-M.M. Millet, Oxidehydrogenation of n-butane over tetravalent metal phosphates based catalysts, Appl. Catal., A,, 227 (2002) 309-320.

[9] B.R. Jermy, B.P. Ajayi, B.A. Abussaud, S. Asaoka, S. Al-Khattaf, Oxidative dehydrogenation of n-butane to butadiene over Bi–Ni–O/γ-alumina catalyst, J. Mol. Catal. A: Chem., 400 (2015) 121-131.

[10] A. Gervasini, Temperature Programmed Reduction/Oxidation (TPR/TPO) Methods, in: A. Auroux (Ed.) Calorimetry and Thermal Methods in Catalysis, Springer Berlin Heidelberg, Berlin, Heidelberg, 2013, pp. 175-195.